Ferrocenyl-terminated polyphenylene-type "click" dendrimers as supports for efficient gold and palladium nanocatalysis

Wenjuan Wang, Elena S. Chamkina, Eduardo Guisasola Cal, Desire Di Silvio, Marta Martinez Moro, Sergio Moya, Jean-René Hamon, Didier Astruc, Zinaida B. Shifrina

▶ **To cite this version:**

Wenjuan Wang, Elena S. Chamkina, Eduardo Guisasola Cal, Desire Di Silvio, Marta Martinez Moro, et al.. Ferrocenyl-terminated polyphenylene-type "click" dendrimers as supports for efficient gold and palladium nanocatalysis. Dalton Transactions, 2021, 50 (34), pp.11852-11860. 10.1039/d1dt01865e . hal-03331243

HAL Id: hal-03331243
https://hal.science/hal-03331243v1

Submitted on 20 Sep 2021

HAL is a multi-disciplinary open access archive for the deposit and dissemination of scientific research documents, whether they are published or not. The documents may come from teaching and research institutions in France or abroad, or from public or private research centers.

L'archive ouverte pluridisciplinaire **HAL**, est destinée au dépôt et à la diffusion de documents scientifiques de niveau recherche, publiés ou non, émanant des établissements d'enseignement et de recherche français ou étrangers, des laboratoires publics ou privés.

Ferrocenyl-terminated polyphenylene-type “click” dendrimers as supports for efficient gold and palladium nanocatalysis

Wenjuan Wang,[a,b] Elena S. Chamkina,[c] Eduardo Guisasola Cal,[d] Desire Di Silvio, [e] Marta Martínez Moro,[d] Sergio Moya,[d] Jean-René Hamon,[b] Didier Astruc [a,*] and Zinaida B. Shifrina [c,*]

a. *Univ. Bordeaux, ISM, UMR CNRS 5255, 33405 Talence Cedex, France. E-mail: didier.astruc@u-bordeaux.fr*

b. *Univ. Rennes, CNRS, ISCR (Institut des Sciences Chimiques de Rennes) – UMR 6226, F-35000 Rennes, France.*

c. *A.N. Nesmeyanov Institute of Organoelement Compounds of Russian Academy of Sciences, Moscow 119991, Russia. E-mail: shifrina@ineos.ac.ru*

d. *Soft Matter Nanotechnology Lab, CIC biomaGUNE, Paseo Miramón 182, 20014 Donostia-San Sebastián, Gipuzkoa, Spain.*

e. *Surface Analysis and Fabrication Platform Manager, Parque Científico y Tecnológico de Gipuzkoa, Paseo Miramón 194, 20014 Donostia / San Sebastián · Gipuzkoa · Spain.*

Abstract: Whereas dendrimer supports are known as key parts of nanocatalysts, the capability of rigid dendrimers for this function has not yet been reported. Here, the study is focused on ferrocenylmethylenetriazolyl-terminated dendrimers (FcMTPD) as supports of remarkably efficient nanogold and nanopalladium catalysts. A biphasic system is elaborated to evaluate the catalytic activity of FcMTPD-supported Au and Pd nanoparticles (NPs) for the reduction of 4-nitrophenol to 4-aminophenol by $NaBH_4$ at 20 °C, and FcMTPD-supported PdNPs are found to be the best nanocatalyst with a rate constant $k_{app}= 7.8\times10^{-2}\ s^{-1}$. Excellent catalytic results are also obtained in this reaction for FcMTPD-supported AuNPs with a rate constant $k_{app}= 5.6\times10^{-2}\ s^{-1}$. For both Pd NPs and AuNPs, the kinetic results are shown to strongly depend on the method of preparation of these NPs that influences the NP size, thus their catalytic efficiency. The FcMTPD-stabilized PdNPs are easily recovered and reused at least 13 times, and their catalytic performance displays only a slight decrease during the first seventh runs.

1. Introduction

The ability of dendrimers[1-4] to stabilize transition-metal nanoparticle catalysts[5-9] has been well recognized. Dendrimers constructed with rigid tethers such as polyphenylene dendrimers[10,11] or poly(azomethine) dendrimers[12,13] present specific structures and

ACCEPTED MANUSCRIPT

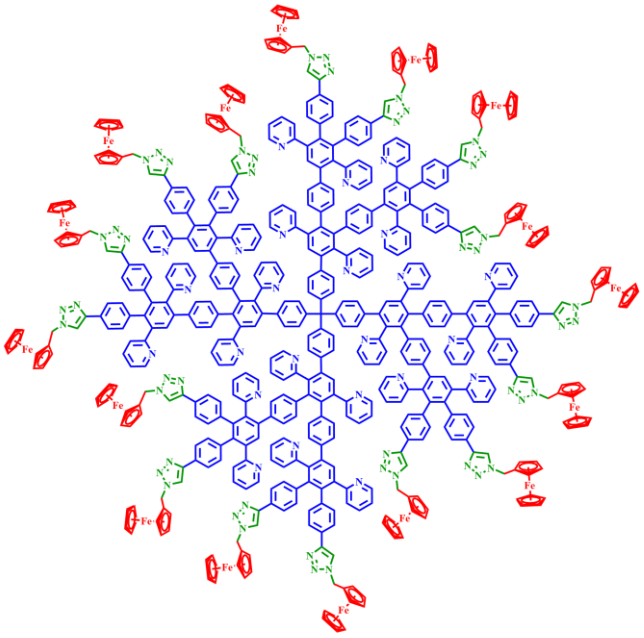

Fig. 1. Structure of the ferrocenylmethylene-triazolyl-poly(phenylene) dendrimer, FcMTPD.

properties that have attracted much attention from researchers. Yamamoto's group has exploited the properties of phenylazomethine dendrimers to stabilize nanoclusters or very small nanoparticles (NPs) that are very active in catalysis,[14,15] but Müllen-type poly(phenylene) dendrimers have not been much utilized for the preparation of active nanocatalysts. Functionalization with pyridyl groups[16] has provided first attempts to coordinate transition metal cations and NPs-,[17,18] with special attention to prion trapping.[19,20] Recently, ferrocene terminated dendrimers with rigid cores have been obtained via the Diels-Alder approach with ferrocene containing cyclopentadienone,[21] and polyphenylene dendrimers containing the pyridyl units and terminated with ethynyl groups have been "clicked" with azidomethyleneferrocene according to the CuAAC reaction to form 1,2,3-triazolylmethylene-ferrocene-terminated poly(phenylene) dendrimers.[22] The later dendrimers possess the 1,2,3-triazole groups near their termini allowing to coordinate transition-metal cations[23-27] and smoothly stabilize late transition-metal NPs. Ferrocene-terminated dendrimers are a well-documented family[28-31] with rich redox properties related to the location of the ferrocene groups in the dendrimers that is favorable toward the use of redox-related processes.[25] Here, the role of the ferrocene termini is to provide bulk at the dendrimer periphery in order to inhibit or at least minimize NP agglomeration, and therefore improve the performances of the nanocatalysts. On the other hand, the ferrocene group does not play any redox role in these catalytic processes, because its reduction would be far too negative to be observed under the reaction conditions. Given the ability of gold[32-34] and palladium[35-

ACCEPTED MANUSCRIPT

[37] NPs as catalysts, we have investigated and report here their stabilization by the ferrocenylmethylene-triazolyl-poly(phenylene) dendrimer (FcMTPD, Fig. 1) and its catalytic properties. The selected reaction in an environmentally-useful process, the prototypical reduction by sodium borohydride of the pollutant nitrobenzene to the nitroaniline dye, an industrial intermediate in the manufacture of analgesic and antipyretic drugs.[38,39] The kinetic of this standard reaction, discovered by Pal and his group upon Ag NP catalysis,[40,41] has been deeply examined by Ballauff and his group,[42-44] and nanocatalysis of nitroarene reduction has been reviewed.[41-45]

2. Results and discussion

2.1. Synthesis and characterization of the metal nanoparticles (MNPs).

FcMTPD was fabricated as described in the literature,[22] and it was used as a stabilizing support of Au(III) and Pd(II) upon reactions with $HAuCl_4$ and Na_2PdCl_4, respectively. The intradendritic triazoles and pyridyls that are present in stoichiometric amount vs. Au(III) displace a chloride ligand from the Au(III) coordination sphere in the mixed solvent system used (CH_2Cl_2/MeOH), so that the main species in aqueous solution is the neutral Au(III) square-planar species [$AuCl_3$(triazole)] or [$AuCl_3$(py)], respectively, as shown earlier with ferrocenyl triazole derivatives.[23-27] Likewise, substitution of a chloride ligand by an intradendritic triazole or pyridyl in $[PdCl_4]^{2-}$ presumably leads to d^8 Pd(II) square-planar species $[Pd(triazole)Cl_3]^-$ or $[PdCl_3(py)]^-$, respectively.[23-27] The lability of the ligands due to the dendritic bulk is not involved, because in such rigid dendrimers the branch termini carrying these ligands are maintained far from one another, unlike in flexible dendrimers. Indeed, the colors and UV-vis. spectra of these solutions were stable for several days.

One hour after addition of the transition-metal salts to the ferrocenylmethylenetriazolyl-terminated dendrimers (FcMTPD)-coordinated Au(III) and Pd(II), addition of $NaBH_4$ rapidly leads to formation of AuNP-1 and PdNP-1 (Scheme 1a). Alternatively, $HAuCl_4$ or Na_2PdCl_4 are added to a mixture of FcMTPD and $NaBH_4$ (Scheme 1b) in the same mixture of solvents, which led to AuNP-2 and PdNP-2. The FcMTPD-supported NPs prepared using these two methods are compared for their plasmon band in the case of the Au NPs and for their size (from TEM measurements) and catalytic activities. In these reduction reactions, the neutral Fe^{II} ferrocenyl groups remain unchanged, because their reduction to Fe^{I} would occur only at extremely negative redox potentials, i. e. around -3 V vs. SCE.[25] This is confirmed by comparison of the XPS analysis of the Fe 2p3/2 orbital of ferrocene in the dendrimer before complexation, after coordination of the dendrimer to Pd(II) and after reduction of Pd(II) by $NaBH_4$ to the Pd(0) NPs. In

ACCEPTED MANUSCRIPT

these three situations, the XPS value for the Fe 2p3/2 orbital remains constant at 707.8 ± 0.1 eV (Table S1, Fig. S1-3), showing that the ferrocene termini, unlike the triazole groups (*vide infra*), are not electronically perturbed by the coordination and reduction processes.

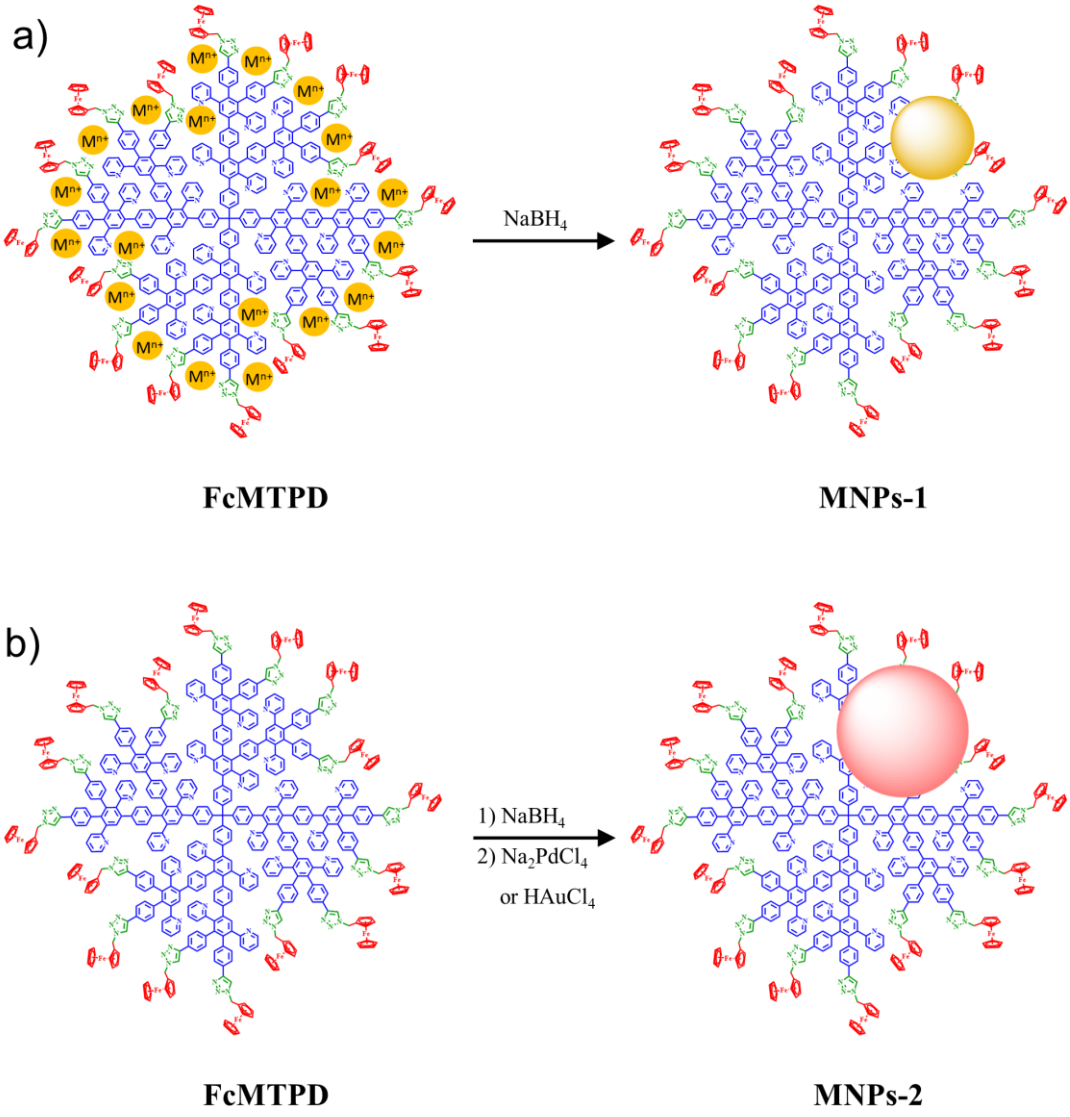

Scheme 1 Syntheses of Au and Pd NPs by a) addition of $NaBH_4$ to FcMTPD-supported Au(III) or Pd(II) leading to the MNPs-1; b) addition of the complex $HAuCl_4$ or Na_2PdCl_4 to a mixture of the dendrimer and $NaBH_4$ leading to the formation of the MNPs-2.

The role of the ferrocene termini is to provide bulk at the dendrimer periphery in order to form a shell around the dendrimer inhibiting encapsulated NP escape. Stabilization of NPs by bulky dendrimer periphery was already observed when three first generations of a dendrimer did not inhibit NPs to escape from inside dendrimers, whereas the fourth

ACCEPTED MANUSCRIPT

generation providing a sufficiently bulky periphery inhibited small NP escape.[17]

During the process of preparation of AuNPs, the color of the CH_2Cl_2 solution changed from light yellow to red-brown for AuNPs-1 and from light yellow to purple for AuNPs-2. The surface plasmon band (SPB) of AuNPs-1 is found at 511 nm and that of AuNPs-2 is observed at 524 nm (Fig. 2). Compared with AuNPs-1, the SPB of AuNPs-2 shows a red shift, qualitatively indicating that AuNPs-2 have a larger size than AuNP-1. For PdNPs, the color of solution changed from yellow-brown to brown for PdNPs-1 and from yellow-brown to golden yellow for PdNPs-2 (Fig. S4).

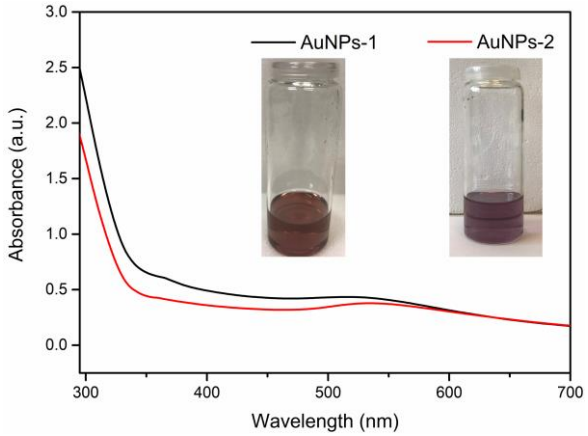

Fig. 2. UV-vis. spectrum of FcMTPD-stabilized AuNPs-1 and AuNPs-2. Insert: photograph of AuNPs-1 (left) and AuNPs-2 (right).

The XPS results show that the FcMTPD-coordinated metal cations have been reduced to metal (0) NPs (Fig. 3). Partial (minor) oxidation to Pd(II) found by XPS (Fig. 3a) is believed to results from some aerobic oxidation occurring between the time of the synthesis and that of the XPS record. Au(0) state in all the FcMTPD-supported AuNPs samples already observed by XPS (Fig. 3b) is confirmed by the presence of the Au plasmon band around 520 nm (*vide supra*, Fig. 2).

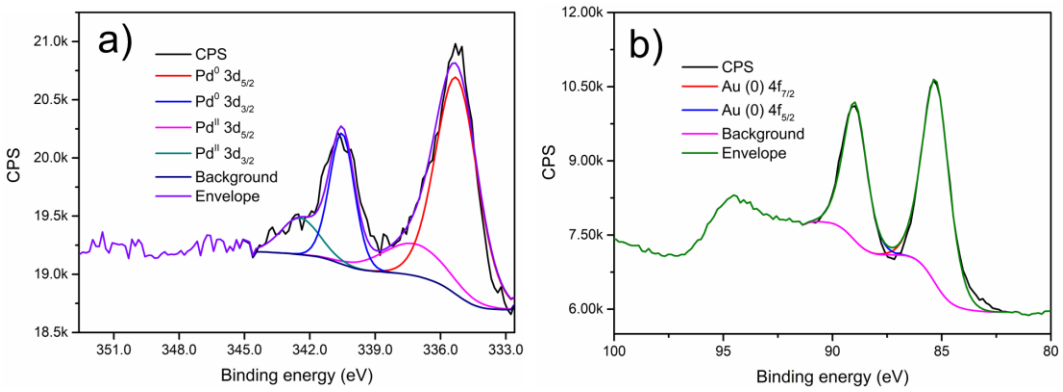

Fig. 3. XPS spectra of the PdNPs-1(a) and AuNPs-1 (b).

ACCEPTED MANUSCRIPT

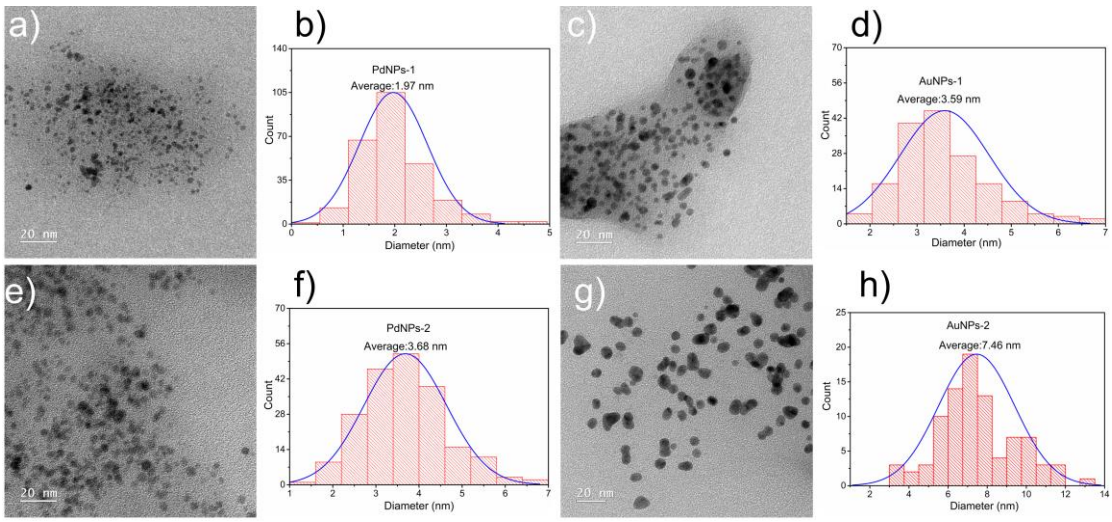

Fig. 4. TEM images of PdNPs-1 (a), AuNPs-1 (c), PdNPs-2 (e) and AuNPs-2 (g); size distribution histogram of PdNPs-1 (b), AuNPs-1 (d), PdNPs-2 (f) and AuNPs-2 (h). The larger size of AuNPs compared to PdNPs is due to the gold aurophilicity involving the relativistic effect of Au atoms facilitating their aggregation.

MNPs with low polydispersity resulting from stabilization by the "click" dendrimer FcMTPD are observed (Fig. 4). The mean sizes of PdNPs-1 and AuNPs-1 are 2.0 nm and 3.6 nm, respectively, and those of PdNPs-2 and AuNPs-2 are 3.7 nm and 7.5 nm, respectively. Compared with AuNPs, PdNPs are smaller, which might be part of the reason explaining why PdNPs show a better catalytic performance than AuNPs. The difference of NP size between the Au and Pd NP synthesized under the same conditions is due to difference of aggregation rates of Pd and Au atoms including the relativistic effect of Au that favors their aggregation in clusters and NPs.[27] In addition, MNPs-2 are larger than MNPs-1, indicating that direct reduction of FcMTPD-supported metal cations to MNPs-1 by $NaBH_4$ is the optimized way to fabricate smaller, more catalytically active MNPs.

The click dendrimers stabilize the NPs through their interaction with the intradendritic triazole rings near their periphery and with pyridines, acting as ligands for the nanoparticle surface. This is beneficial for catalysis, because large agglomerated NPs would be less catalytically active.[4] NPs Indeed, earlier comparison between click dendrimers containing triazole ligands near their periphery and dendrimers of similar size that did not contain triazole groups showed that only triazole-containing dendrimers near their periphery stabilized such small nanoparticles, whereas other dendrimers stabilized only very large nanoparticles (like 10 nm).[46,47] By analogy, the fact that relatively small NPs were characterized here confirm the existence of these dendrimer-NP interactions that occur necessarily at the dendrimer peripheries, given the closely related sizes of the dendrimer and NPs. Nevertheless, since the dendritic

ACCEPTED MANUSCRIPT

triazoles and pyridines appear to be the ligands stabilizing the NPs, this implies a small penetration of the NPs near the external part of the dendrimers. These tether extremities can bend (unlike the rigid interiors), because the triazolyl ferrocenes are the only flexible fragments of the dendrimer. [46,47]

XPS analysis of the N atoms provides useful information on the coordination of the N-containing intradendritic ligands by Pd(II) upon reaction with Na_2PdCl_4 and Pd(0) NPs formed upon reduction of the former by $NaBH_4$.[48] The compared XPS data of the N 1s orbital of FcMTPD alone, Pd(II)-FcMTPD complexes and Pd(0)NPs-FcMTPD are shown in Figure 5. In the Pd(II)-dendrimer complex, the very significant shift of the N 1s binding energy to a higher value shows the electron-donating effect from N to Pd(II) due to the N atoms sharing their lone pairs with Pd(II). With the Pd(0) NP complex, this shift is much weaker as expected due to the much weaker electronic donation from N to Pd(0) than with Pd(II), although it can still clearly be observed.

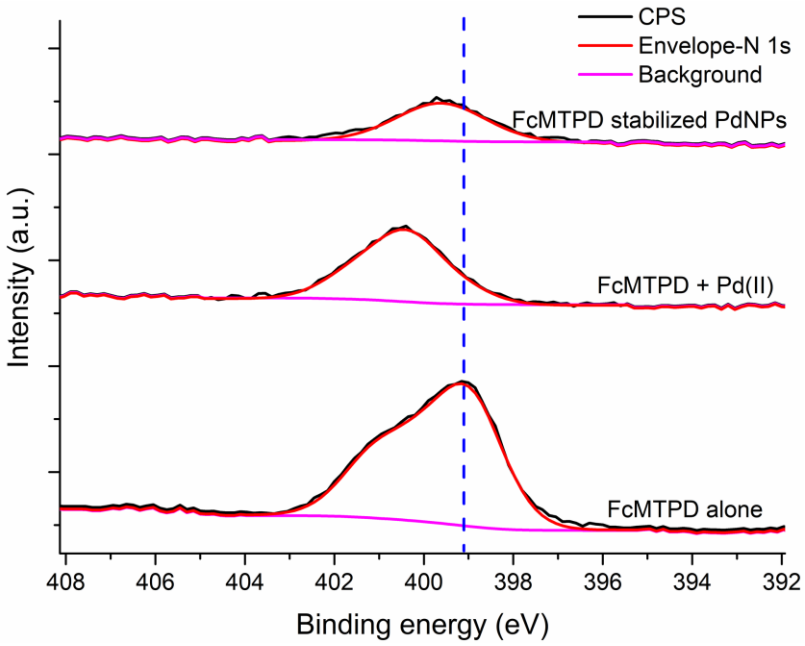

Fig. 5. N 1s XPS of FcMTPD alone, Pd(II)-FcMTPD and Pd(0) NP@FcMTPD.

2.2. Catalysis by the metal NPs of 4-nitrophenol (4-NP) reduction.

The catalytic activity of metal NPs (MNPs) for the 4-nitrophenol (4-NP) reduction to 4-aminophenol (4-AP) was evaluated using a standard reaction, the reduction of 4-NP to 4-AP by $NaBH_4$. This reaction, disclosed by Pal group in 2002, has been much studied mechanistically,[42-45] and the intermediacy of nitrosophenol and 4-hydroxyaminophenol has been shown.[41] Several mechanisms including the Langmuir-Hinshelwood mechanism with fast adsorption of both substrates on the catalyst, discussed through in-depth studies by Ballauff,[42] and the Eley-Rideal mechanism

ACCEPTED MANUSCRIPT

involving hydride adsorption[41] have been proposed. Indeed, metal NPs behave as electron reservoirs[49-51] with surface atom-hydrogen bond intermediates,[49,51] and the hydride donor $NaBH_4$ has been shown to be able to transfer sequentially an electron and a hydrogen atom to delocalized electron-reservoir systems[51] such as late transition-metal NPs. Likewise, the hydride transfer steps from the NP catalyst to 4-NP can proceed by a sequence of electron transfer followed by hydrogen atom transfer, coupled electron-hydrogen atom transfer[52] or direct hydride transfer. Activation of the NP surface-adsorbed nitrophenolate substrate in the rate-limiting step is then all the easier as the NP catalyst is negatively charged, which increases its reactivity.[53,54] The convenience of the 4-NP reduction reaction is due to its simple manipulation and obvious color change during the reaction process. In addition, whereas the reaction is usually conducted in water only, a biphasic system composed of CH_2Cl_2 and water was newly used here in order to carry out the catalytic reaction, since both the dendrimer and the MNPs are soluble in CH_2Cl_2. Therefore, in the reaction mixture, the MNP catalyst is located in the lower layer (CH_2Cl_2 phase) and the substrates are located in the upper layer (aqueous phase). The color of the aqueous solution containing 4-NP changes from pale yellow to dark yellow upon addition of $NaBH_4$, owing to the formation of sodium 4-nitrophenolate. After the reaction is completely finished, the dark-yellow color vanishes, and therefore the reaction mixture becomes colorless.

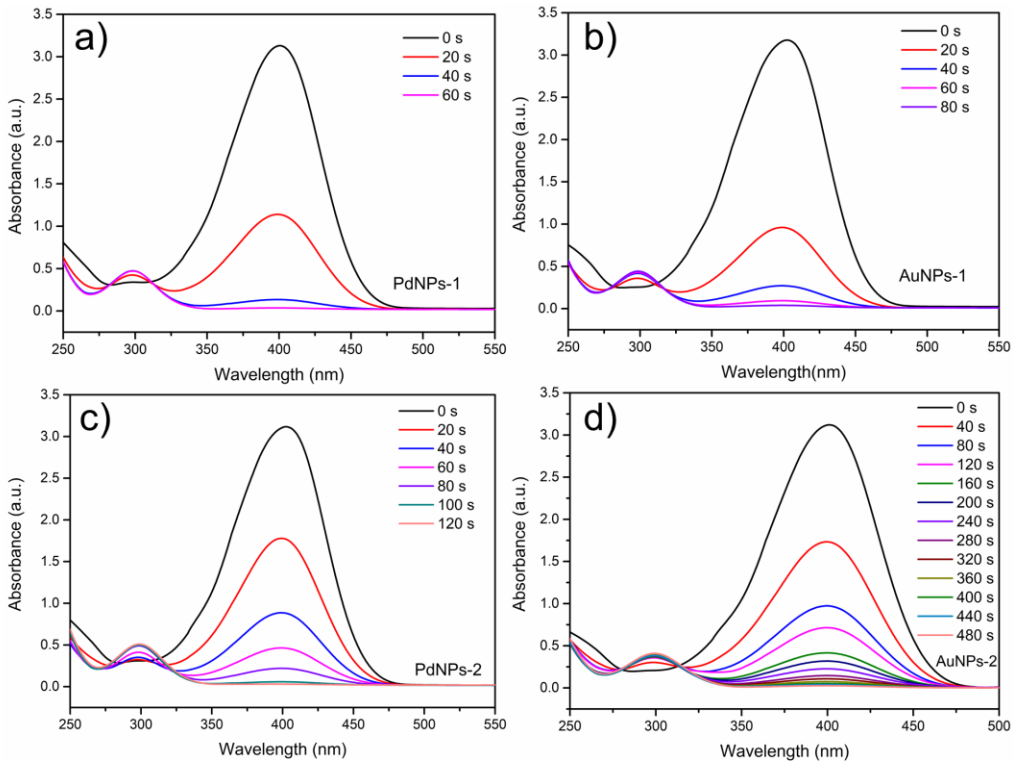

Fig. 6. Time-dependent UV-vis. spectrum of *p*-nitrophenol reduction in the presence of different catalysts (0.5% mmol of MNPs).

ACCEPTED MANUSCRIPT

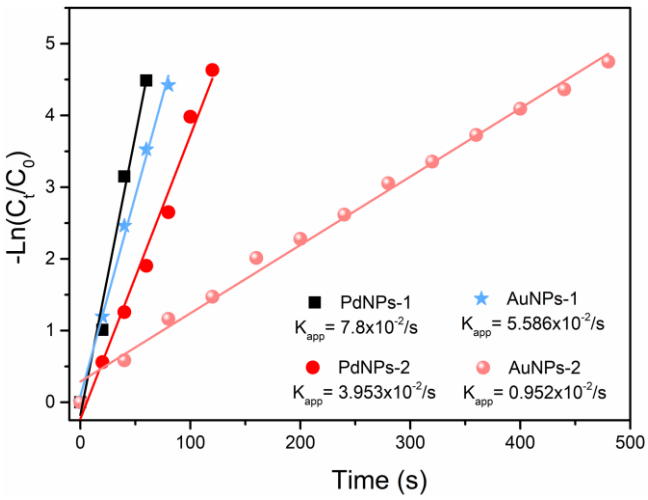

Fig. 7. Plots of the consumption rate of 4-NP: [-ln (C_t/C_0)] *vs.* reaction time with 0.5% mmol of nanocatalyst. See ESI (eq. 7 and Table S2) for the calculation of the rate constant normalized to the surface of the particles in the medium.[42,43]

As shown in Fig. 6a, with 0.5% mmol of PdNPs-1, the absorbance peak at 400 nm corresponding to the nitrophenolate anion decreases rapidly with time and disappears after 60 s, with a k_{app}= (7.8 ± 0.7) × 10^{-2} s^{-1} (Fig. 7). A weak signal at 300 nm corresponding to 4-AP appears, and its intensity gradually increases with time. Under the same conditions, for AuNPs-1 (Fig. 6b), it takes 80 s to finish the catalytic reaction, and the value of the rate constant k_{app} is (5.6 ± 0.2) ×10^{-2} s^{-1} (Fig. 7). In addition, no more absorption band at 400 nm is observed after 120 s for PdNPs-2 (Fig. 6c) and 480 s for AuNPs-2 (Fig. 6d), and their values of k_{app} are (4.0 ± 0.2) ×10^{-2} s^{-1} and (0.95 ± 0.02) ×10^{-2} s^{-1} (Fig. 7), respectively. Compared to the other MNPs, PdNPs-1 is the best catalyst for the reduction of 4-NP. The comparison between MNPs-1 and MNPs-2 shows the higher catalytic efficiency of MNPs-1. This efficiency difference between MNPs-1 and MNPs-2 is more marked for AuNPs-1 whose catalytic efficiency is around 6 times as much as that of AuNPs-2. This result signifies that the synthetic method of preparation of MNPs-1 by addition of $NaBH_4$ into a solution containing both the dendrimer and the metal salt is superior to that involving addition of metal salt into a mixture of the dendrimer and $NaBH_4$. The lower catalytic efficiency of MNPs-2 is attributed to the lack of complete coordination of the metal cation with the dendritic triazole during the short reaction time followed by rapid reduction to MNPs-2 in large part in solution outside the FcMTPD. This results in inter-FcMTPD NP stabilization of MNPs-2 rather than intra-FcMTPD NP stabilization in the case of MNPs-1. Outside the dendrimer, the reduced steric confinement let NP aggregation proceed further before inter-FcMTPD NP stabilization. As a consequence, the MNPs-2 are larger than the MNPs-1 and less catalytically active, because the total surface of MNPs-2 is smaller than that of MNPs-1 for the same mass amount. The presence of the bulky terminal

ACCEPTED MANUSCRIPT

ferrocenyl group apparently serves to optimize the balance between stabilization and catalytic activity.

The remarkably low polydispersity of the NPs and the NP stability and small size (2 to 4 nm) related to that of the dendrimer (4 nm) all confirm encapsulation near the periphery of the dendrimers (*vide infra*) and stabilization by coordination of the intra-dendritic triazole. The interaction of the NP with the bipyridine ligands did not lead to improvement of the catalytic reactions upon increasing the amount of metal precursor in order to account for pyridine coordination (Fig. S5-S7).

As shown in Fig. S9, with 0.5% mmol of MNPs-3, no signal at 400 nm is observed after 80 s for PdNPs-3 (Fig. S6a) and 120 s for AuNPs-3 (Fig. S6b), and their k_{app} values are $(7.1 \pm 0.5) \times 10^{-2}$ s^{-1} and $(4.4 \pm 0.6) \times 10^{-2}$ s^{-1} (Fig. S6c), respectively. In addition, MNPs-3 will cluster and form precipitation after 2 h for AuNPs-3 (Fig. S7a and b) and 12 h for PdNPs-3 (Fig. S7c). These results suggest that the catalytic performance and stability of MNPs-3 are not as good as those of MNPs-1, and a weaker interaction between the pyridine ligands and MNPs.

The comparison of the apparent rate constants k_{app} observed here with those recently reported in the literature shows the excellent efficiency of the present FcMTPD-supported Au and Pd NPs (Table 1).

Table 1 Comparison of selected literature apparent rate constants k_{app} with the present results for the nanocatalyzed reduction of 4-NP to 4-AP by $NaBH_4$.

Entry	Catalyst	Catalyst amount (ug)	k_{app} (s^{-1})	Reference
1	Pure Pt	4.0	1.25×10^{-4}	55
2	Raney Ni	4.0	1.48×10^{-4}	55
3	NiPt NPs	4.0	1.93×10^{-3}	54
4	PtPdFe	2.5	3.00×10^{-2}	56
5	PdCuFe/RGO	2.8	8.90×10^{-3}	56
6	Pd/RGO	2.5	4.52×10^{-3}	56
7	PtCu/RGO	2.6	8.02×10^{-3}	56
8	Pd	3.1	1.02×10^{-3}	56
9	Pd/AC	3.0	2.58×10^{-2}	56
10	AuNP-5	5.2	2.63×10^{-2}	57
11	AuNP-5	1.3	1.33×10^{-2}	57
12	PdNPs-1	0.7	$(7.8 \pm 0.7) \times10^{-2}$	This work
13	AuNPs-1	1.3	$(5.6 \pm 0.2)\times10^{-2}$	This work

ACCEPTED MANUSCRIPT

2.3. Stability of PdNPs-1 in the reduction of 4-NP

To further assess the catalytic activity of MNPs, the best catalyst PdNPs-1 was selected to check its recyclability. After the catalytic reduction of 4-NP was completely finished, the biphasic system was kept still until the organic phase and aqueous phase were well separated. The catalyst PdNPs-1 in the lower CH_2Cl_2 phase was recovered by removing the aqueous solution with 4-AP. A fresh aqueous solution of 4-NP and $NaBH_4$ was added into the reused catalyst solution for another round of reaction as shown in Fig. 8a. The reaction time for full conversion of 4-NP changed with increase of the number of recycling (Fig. 8b). The catalytic performance exhibited a slight decrease from the 1st run to 7th run, but showed an obvious decrease after the 11th run, which is ascribed to the tendency of PdNPs-1 tend to aggregate. However, PdNPs-1 still display a good catalytic activity even after being reused 13 times.

After the 1st cycle, the size of the AuNPs-1 displays a change from 4 nm to 7.46 nm but that of PdNPs-1 changes a little bit from 2 nm to 2.95 nm (Fig. S8). Besides, the UV-vis. spectrum of PdNPs-1 keeps the same shape, but the SPB of AuNPs-1 shows a red shift from 511 nm to 540 nm (Fig. S9), revealing that AuNPs-1 with larger size tend to aggregate after the 1st run, which is in concordance with the TEM images. Thus, the stability of PdNPs-1 is much better than that of AuNPs-1.

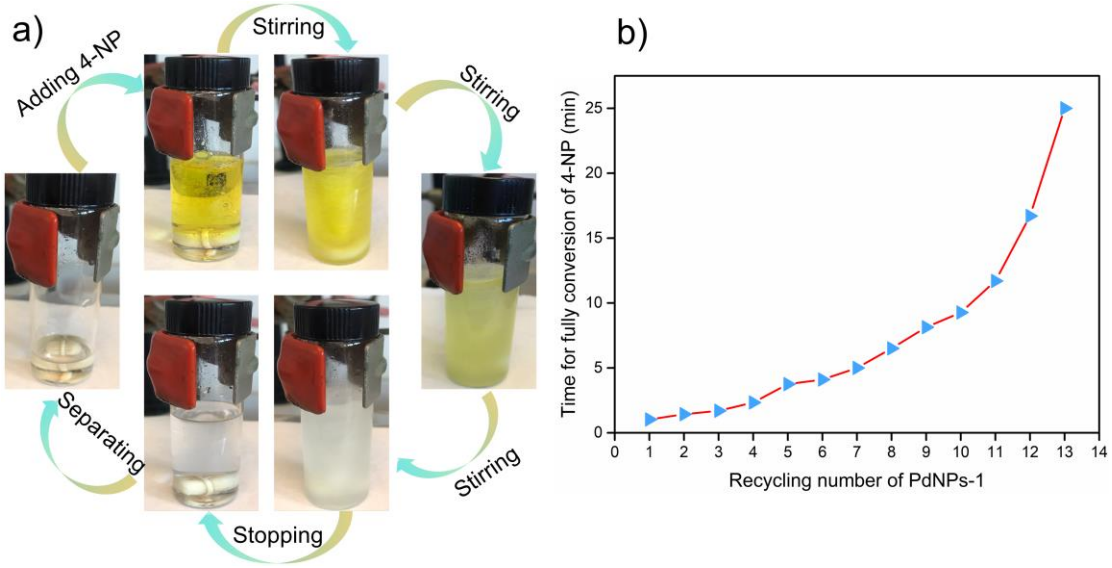

Fig. 8. (a) Schematic diagram for the re-use of PdNPs-1 in the reduction of 4-NP. Plots of reaction time for full conversion vs. recycling number of PdNP-1 (b).

ACCEPTED MANUSCRIPT

3. Experimental Section

3.1. Synthesis of MNPs-1 stabilized by FcMTPD.

FcMTPD was prepared according to the literature procedure by copper-catalyzed azide-alkyne cycloaddition (CuAAC) reaction between a previously reported ethynyl-terminated dendrimer and azidomethylferrocene.[22] Then, a solution (V_{CH2Cl2}/ V_{MeOH} = 30:1, 6.8 mL) of Na_2PdCl_4 (or $HAuCl_4$, 1.0×10^{-3} mmol, n_{metal}:n_{trz} = 1:1) was mixed with a solution (V_{CH2Cl2}/ $V_{methanol}$ = 30:1, 3 mL) of the dendrimer FcMTPD (6.25×10^{-5} mmol) in a 20 mL flask with a stir bar. After the mixture was stirred for 30 min, then 5.0×10^{-3} mmol of $NaBH_4$ was added into the flask under vigorous stirring. After continuous stirring for 1 h at room temperature, the metal nanoparticles were obtained.

3.2. Synthesis of MNPs-2 stabilized by FcMTPD.

A solution (V_{CH2Cl2}/ $V_{methanol}$ = 30:1, 3.2 mL) of FcMTPD (6.25×10^{-5} mmol) and $NaBH_4$ (5.0×10^{-3} mmol), and a stir bar were introduced into a 20 mL flask, then a solution (V_{CH2Cl2}/ V_{MeOH} = 30:1, 6.8 mL) of the Na_2PdCl_4 (or $HAuCl_4$, 1.0×10^{-3} mmol, n_{metal}:n_{trz} = 1:1) was added dropwise under vigorous stirring. After continuous stirring for 1 h at room temperature, the MNPs were obtained.

3.3. Reduction of 4-NP to 4-AP catalyzed by MNPs-1 and MNPs-2

First, a fresh solution of MNP (0.5% mmol) was injected into a 20 mL flask, and CH_2Cl_2 was added until the volume of organic phase reached 3 mL. Then a 10 mL prepared aqueous solution of 4-NP (4.17 mg, 3.0×10^{-2} mmol) and $NaBH_4$ (113.5 mg, 3.0 mmol) were added into the flask.[57] Then, the reaction system was vigorously stirred at rt. The dark-yellow color of the mixture changed to colorless with time, and UV−vis. spectroscopy was applied to monitor the process of the reaction kinetics (40 s for each round).

3.4. Recycling of PdNPs-1 for 4-NP reduction

Catalytic reduction of 4-NP by PdNPs-1 was recorded according to the steps mentioned above. While the color of the mixture became colorless, the biphasic system was kept still until the organic phase and aqueous phase were completely separated. The CH_2Cl_2 phase with the catalyst PdNPs-1 was recovered by removing the aqueous solution with

ACCEPTED MANUSCRIPT

4-AP. In order to keep the volume of CH_2Cl_2 at 3 mL, fresh CH_2Cl_2 was injected into the biphasic system to reach this volume. 10 mL of fresh aqueous solution of 4-NP and $NaBH_4$ was added into the reused catalyst solution for another round of reaction.

4. Conclusion

In summary, the FcMTPD containing 1,2,3-triazolyl and pyridyl groups was used to stabilize PdNPs and AuNPs. Two preparation modes were compared for both metal NPs in order to optimize the FcMTPD-supported NP catalytic efficiency, and it was found that addition of $NaBH_4$ addition to pre-coordinated metal cation leading to MNPs-1 provided the best results. MNPs-2 prepared by addition of the metal cation complex to a solution containing a mixture of FcMTPD and $NaBH_4$ produced less efficient PdNPs-2 and AuNPs-2, respectively than the corresponding MNPs-1, which was assigned to increased aggregation of MNPs-2 outside FcMTPD. Whereas this reaction is usually conducted in water, a new biphasic system was elaborated here to evaluate the catalytic activity of FcMTPD-supported MNPs-1 and MNPs-2 in the reduction of 4-NP to 4-AP by $NaBH_4$ at 20 °C. Such a new biphasic system involving hydrophobic nanocatalysts that are insoluble in water is extremely practical and could in principle be extended in the future to any other hydrophobic nanocatalyst.[58] For instance, the catalytic efficiency of AuNPs-1 was around 6 times superior to that AuNPs-2 in terms of rate constant k_{app}. This result indicates that the location of small MNPs supported by the nitrogen ligands inside the periphery of the FcMTPD plays a vital role for the NP catalytic efficiency. Although the dendritic core of FcMTPD is rigid, the bulky terminal CH_2Fc group can freely rotate around the triazole-CH_2 bond to accommodate adequate coordination of the ligands to transition metal cations and, more smoothly, to NPs for their stabilization. In this way a reasonable balance is obtained between NP stabilization and catalytic activity. As a result, the FcMTPD-stabilized PdNPs show excellent catalytic efficiency and stability, as indicated by recycling using the biphasic system. Indeed, the catalytic activity of these PdNPs-1 exhibits only a slight decrease, allowing the system to be reused many times.

5. Acknowledgements

Financial support from the China Scholarship Council (CSC, PhD grant to W. W.), the Universities of Rennes 1 and Bordeaux, the Centre National de la Recherche Scientifique (CNRS), the Ministry of Science and Higher Education of the Russian Federation using the equipment of Center for molecular composition studies of INEOS RAS, and CIC biomaGUNE is gratefully acknowledged.

ACCEPTED MANUSCRIPT

6. Conflict of interest

There are no conflicts of interest.

7. References

1. D. A. Tomalia, *Molecules*, 2016, **21**, 1035.
2. G. R. Newkome, C. N. Morefield and S. Chakraborty, *J. Inorg. Organomet. Polym. Mater.*, 2018, **28**, 360-368.
3. S. Mignani, J. Rodrigues, H. Tomas, M. Zabloka, X. Y. Shi, A. M. Caminade and J.-P. Majoral, *Chem. Soc. Rev.*, 2018, **47**, 514-532.
4. D. Astruc, E. Boisselier and C. Ornelas, *Chem. Rev.*, 2010, **110**, 1857-1959.
5. R. M. Crooks, M. Q. Zhao, L. Sun, V. Chechik and L. K. Yeung, *Acc. Chem. Res.*, 2001, **34**, 181-190.
6. R. W. J. Scott, O. M. Wilson and R. M. Crooks, *J. Phys. Chem.*, 2005, **109**, 692-704.
7. Z. D. Pozun, S. E. Rodenbusch, E. Keller, K. Tran, W. J. Tang, K. J. Stevenson and G. Henkelman, *J. Phys. Chem. C*, 2013, **117**, 7598-7604.
8. G. R. Newkome and C. Shreiner, *Chem. Rev.*, 2010, **110**, 6338-6442.
9. D. Wang, C. Deraedt and D. Astruc, *Acc. Chem. Res.*, 2015, **48**, 1871-1880.
10. F. Morgenroth, E. Reuther and K. Müllen, *Angew. Chem., Int. Ed. Engl.*, 1997, **36**, 631-634.
11. A. J. Berresheim, M. Müller and K. Müllen, *Chem. Rev.*, 1999, **99**, 1747-1785.
12. M. Higushi, S. Shiki and K. Yamamoto, *Org. Lett.*, 2000, **2**, 3079-3082.
13. M. Higushi, S. Shiki, K. Ariga and K. Yamamoto, *J. Am. Chem. Soc.*, 2001, **123**, 4414-4420.
14. K. Yamamoto, T. Imaoka, M. Tanabe and T. Kambe, *Chem. Rev.*, 2020, **120**, 1397-1437.
15. T. Moriai, T. Tsukamoto, M. Tanabe, T. Kambe and K. Yamamoto, *Angew. Chem., Int. Ed.*, 2020, **59**, 23051-23055.
16. Z. B. Shifrina, M. S. Averina, N. V. Firsova, A. L. Rusanov and K. Muellen, *Dokl. Chem.,* 2005, **400**, 34−38.
17. Z. B. Shifrina, M. S. Rajadurai, N. V. Firsova, L.M. Bronstein, X. Huang, A. L. Rusanov and K. Muellen, *Macromolecules*, 2005, **38**, 9920−9932.
18. E. Y. Yuzik-Klimova, N. V. Kuchkina, S. A. Sorokina, D. G. Morgan, B. Boris, L. Z. Nikoshvili, N. A. Lyubimova, V. G. Matveeva, E. M. Sulman, B. D. Stein, W. E. Mahmoud, A. A. Al-Ghamdi, A. Kostopoulou, A. Lappas, Z. B. Shifrina and L. M. Bronstein, *RSC Adv.*, 2014, **4**, 23271−23280.
19. S. Sorokina, P. Semenyuk, Y. Stroylova, V. Muronetz and Z. Shifrina, *RSC Adv.*, 2017, **7**, 16565−16574.
20. S. A. Sorokina, Y. Y. Stroylova, Z. B. Shifrina and V. I. Muronetz, *Macromol. Biosci.*, 2016,

ACCEPTED MANUSCRIPT

16, 266−275.

21. E. S. Serkova, A. A. Chamkin, K. L. Boldyrev, V. V. Novikov, A. S. Peregudov and Z. B. Shifrina, *Polymer*, 2019, **173**, 34−42.
22. E. S. Serkova, A. A. Chamkin, K. L. Boldyrev and Z. B. Shifrina, *Macromolecules*, 2020, **53**, 2735-2743.
23. S. Badèche, J.-C. Daran, J. Ruiz and D. Astruc, *Inorg. Chem*., 2008*, **47,*** 4903-4908。
24. F. A. Cotton, G. Wilkinson, C. A. Murillo, M. Bochmann, *Advanced Inorganic Chemistry*, 6th Ed, Wiley, New York, 1999, p. 1063 for square planar d^8 $[Pd^{II}LCl_3]^-$, and p.1101 for square planar d^8 $[Au^{III}LCl_3]$, L = 2-electron, neutral donor ligand.
25. D. Astruc, *Eur. J. Inorg. Chem*. 2017, 6-29.
26. C. A. P. Goodwin, M. J. Gianciracusa, S. M. Greer, H. M. Nicholas, P. Evans, M. Vonci, S. ill, N. F. Shilton and D. P. Mills, *Nat. Chem*., 2021, **13**, 243–248.
27. P. Pyykkö and J. P. Desclaux*, Acc. Chem. Res.,* 1979, **12**, 276-281.
28. C. M. Casado, I. Cuadrado, M. Morán, B. Alonso, B. Garcia, B. González and J. Losada, *Coord. Chem. Rev.*, 1999, **185−186**, 53−80.
29. C. M. Casado, B. Alonso, J. Losada, and M. P. Garcia-Armada, in *Designing Dendrimers*, S. Campagna, P. Ceroni and F. Puntoriero, Eds., Wiley, Hoboken, NJ, USA, 2012, 219-262.
30. C. Ornelas, J. Ruiz, C. Belin and D. Astruc, *J. Am. Chem. Soc*., 2009, ***131***, 590-601.
31. D. Astruc, *Nat. Chem.*, 2012, **4**, 255-267.
32. T. Ishida, T. Murayama, A. Taketoshi and M. Haruta, *Chem. Rev.* 2020, **120**, 464-525.
33. M. Sankar, Q. He, R. V. Engel, M. A. Sainna, A. J. Logsdail, A. Roldan, D. J. Willock, N. Agarwal, C. J. Kiely and G. J. Hutchings, *Chem. Rev.*, 2020, **120**, 3890-3938.
34. M.-C. Daniel and D. Astruc, *Chem. Rev.* 2004, **104**, 293-346.
35. N. T. S. Phan, M. Van der Sluys and C. W. Jones, *Adv. Syn. Catal.*, 2006, **348**, 609-679.
36. M. T. Reetz and J. G. de Vries, *Chem. Commun.* 2004, 1559-1563.
37. D. Astruc, F. Lu and J. Ruiz, *Angew. Chem., Int. Ed***.** 2005, **44**, 7852-7872;
38. A. Olaniran, O. Ademola and E. O. Igbinosa, *Chemosphere*, 2011, **83**, 1297-1306.
39. F. Lu and D. Astruc, *Coord. Chem. Rev*., **2020**, 408, 213180.
40. N. Pradhan, A. Pal and T. Pal, *Colloids Surf. A-Physicochem. Eng. Asp.*, 2002, **196**, 247-257.
41. T. Aditya, A. Pal and T. Pal, *Chem. Commun.* 2015, **51**, 9410-9431.
42. S. Wunder, F. Polzer, Y. Lu, Y. Mei and M. Ballauff, *J. Phys. Chem. C* 2010, **114**, 8814-8820.
43. P. Herves, M. Perez-Lorenzo, L. M. Liz-Marzan, J. Dzubiella, Y. Lu and M. Ballauff, *Chem. Soc. Rev.* 2012, **41**, 5577-5587.
44. Y. Lu and M. Ballauff, *Prog. Polym. Sci.* 2015, **59**, 86-104.
45. P. Zhao, X. Feng, D. Huang and D. Astruc, *Coord. Chem. Rev.* 2015, **287**, 114-136.
46. Y. Wang, L. Salmon, J. Ruiz and D. Astruc, *Nat. Commun*. 2014, **5**, 3489.
47. X. Liu, D. Gregurec, J. Irigoyen, A. Martinez, S. Moya, R. Ciganda, P. Hermange, J. Ruiz

ACCEPTED MANUSCRIPT

and D. Astruc, *Nat. Commun*. 2016, **7**, 13152.
48. J. Yang, E. H. Sargent, S. Kelley, and J. Y. Ying, *Nat. Mater*. 2009, 8, 683-689.
49. R. Ciganda, N. Li, C. Deraedt, S. Gatard, P. Zhao, L. Salmon, R. Hernandez, J. Ruiz, and D. Astruc, *Chem. Commun.* 2014, **50**, 10126-10129.
50. M.-H. Desbois, D. Astruc, J. Guillin, F. Varret, A. X. Trautwein and G. Villeneuve, *J. Am. Chem. Soc.* 1989, **111**, 5800-5809.
51. P. Michaud, D. Astruc and J.-H. Ammeter, *J. Am. Chem. Soc*. 1982, **104**, 3755-3757.
52. A. Migliore, N. F. Polizzi, M. J. Therien and D. N. Beratan, *Chem. Rev*., 2014, **114**, 3381-3465.
53. C. Nero, H. J. Peterson and G. S. Saines, *Chem. Rev*. 1960, **60**, 7-14.
54. W. Y. Ai, R. Zhong, X. F. Liu and Q. Liu, *Chem. Rev*. 2019, **119**, 2876-2953.
55. S.K. Ghosh, M. Mandal, S. Kundu, S. Nath and T. Pal, *Appl. Catal. A* 2004, **268**, 61–66.
56. S.J. Hoseini, M. Bahrami, N. Sadri, N. Aramesh, Z. Samadi Fard, H. Rafatbakhsh Iran, B. Habib Agahi, M. Maddahfar, M. Dehghani, A. Zarei Baba Arabi, N. Heidari, S.F. Hashemi Fard and Z. Moradi, *J. Coll. Interf. Sci.* 2018, **513**, 602–616.
57. F. F. Liu, X. Liu, D. Astruc and H. Gu, *J. Colloid Interfac. Sci.* 2019, **533**, 161-170.
58. D. Astruc, K. Heuze, S. Gatard, *Adv. Syn. Catal*. 2005, **347**, 329-338.

ACCEPTED MANUSCRIPT